

OFDM and FBMC-OQAM in Doubly-Selective Channels: Calculating the Bit Error Probability

Ronald Nissel, *Student Member, IEEE* and Markus Rupp, *Fellow, IEEE*

Abstract—Filter Bank Multi-Carrier (FBMC) is a modulation technique with enhanced spectral properties compared to Orthogonal Frequency Division Multiplexing (OFDM). In this letter, we investigate the performance degeneration of OFDM and FBMC in doubly-selective channels, that is, time-selectivity and frequency-selectivity. For that, we derive closed-form Bit Error Probability (BEP) expressions for arbitrary linear modulation methods based on one-tap equalizers, with OFDM and FBMC being special cases, covered by our general BEP expressions. We validate our calculations by Monte-Carlo simulations and investigate the BEP error if the interference is approximated as Gaussian noise.

Index Terms—FBMC, OFDM, Bit Error Probability, Multipath channels, Time-varying channels.

I. INTRODUCTION

FUTURE wireless systems should support a large range of possible use cases, such as high data rates, machine-to-machine communications and low-latency transmissions. This requires a flexible assignment of the available time-frequency resources, not possible in conventional Orthogonal Frequency Division Multiplexing (OFDM) due to its poor spectral behavior. For such diverse applications, Filter Bank Multi-Carrier (FBMC) [1] becomes an efficient alternative to OFDM due to much better spectral properties. In this letter, we consider FBMC based on Offset Quadrature Amplitude Modulation (OQAM), in short just FBMC, because it achieves maximum spectral efficiency. Although the integration of Multiple-Input and Multiple-Output (MIMO) in FBMC is not as straightforward as in OFDM due to the intrinsic imaginary interference, there exist methods which allow an efficient implementation of MIMO [2], making it a viable choice for future wireless systems.

Of particular interest is the comparison of different modulation schemes in time-variant multipath propagation, i.e., time-selectivity and frequency-selectivity, in short, doubly-selectivity. An important metric for the comparison is the Bit Error Probability (BEP). Many authors have already investigated the BEP in OFDM from an analytical point of view,

Manuscript received xxxx; accepted xxxx. Date of publication xxxx; date of current version xxxxx.

The financial support by the Austrian Federal Ministry of Science, Research and Economy, the National Foundation for Research, Technology and Development, and the TU Wien is gratefully acknowledged. This work has been co-funded by A1 Telekom Austria AG, Kathrein Werke KG and Nokia Solutions and Networks. The associate editor coordinating the review of this manuscript and approving it for publication was xxxxx.

The authors are with the Christian Doppler Laboratory for Dependable Wireless Connectivity for the Society in Motion, Institute of Telecommunications, TU Wien, 1040 Vienna, Austria (e-mail: rnissel@nt.tuwien.ac.at; mrupp@nt.tuwien.ac.at).

Digital Object Identifier: xxx.

such as [3] for a time-invariant channel and [4] for a doubly-selective channel. However, FBMC is still missing in literature, motivating our paper.

In this letter, we propose a compact framework to calculate the BEP in doubly-selective channels for arbitrary linear modulation techniques based on one-tap equalizers, such as OFDM or FBMC. We assume Rayleigh fading, perfect channel knowledge at the receiver and that the data symbols are chosen from a m -Quadrature Amplitude Modulation (QAM) or \sqrt{m} -Pulse-Amplitude Modulation (PAM) signal constellation, but the bit mapping can be arbitrary.

Note that the MATLAB code used in this paper can be downloaded at <https://www.nt.tuwien.ac.at/downloads/> and supports reproducibility of our results.

II. SYSTEM MODEL

In multi-carrier transmissions, symbols are usually transmitted over a rectangular time-frequency grid. Let us denote the transmit data symbol at subcarrier position l and time-position k by $x_{l,k} \in \mathcal{A}$ with \mathcal{A} denoting the symbol alphabet, for example QAM or PAM. The transmitted signal $s(t)$, consisting of L subcarriers and K time-symbols, then becomes

$$s(t) = \sum_{k=1}^K \sum_{l=1}^L g_{l,k}(t) x_{l,k}, \quad (1)$$

whereas the basis pulses $g_{l,k}(t)$ are, essentially, time and frequency shifted versions of the prototype filter $p(t)$:

$$g_{l,k}(t) = p(t - kT) e^{j2\pi l F (t - kT)} e^{j\theta_{l,k}}. \quad (2)$$

Note that time spacing T and frequency spacing F determine the spectral efficiency. Unfortunately, it is not possible to find basis pulses which have a time-frequency spacing of $TF = 1$, are localized in both, time and frequency, and are orthogonal, according to the Balian-low theorem [5]. At least one of these desired properties has to be sacrificed. In pure OFDM, $p(t)$ is a rectangular function, violating frequency-localization. Additionally, a Cyclic Prefix (CP) is often added in OFDM to improve robustness in frequency-selective channels, decreasing the spectral efficiency ($TF = 1 + T_{\text{CP}}F > 1$). FBMC, on the other hand, usually employs a prototype filter $p(t)$ which is localized in both, time and frequency, for example based on Hermite polynomials [6]. Such prototype filter is orthogonal for $TF = 2$. The time spacing as well as the frequency spacing is then reduced by a factor of two, leading to $TF = 0.5$. This causes interference which, however, is shifted to the purely imaginary domain by selecting the phase shift as $\theta_{l,k} = \frac{\pi}{2}(l + k)$. Because of the imaginary interference,

only real valued symbols can be transmitted, so that two real valued symbol are required to transmit one complex symbol, leading to the same information rate as OFDM without CP, that is $TF = 1$. Thus, FBMC satisfies the Balian-low theorem by replacing the complex orthogonality condition with the less strict real orthogonality condition.

To simplify analytical investigations, we consider a time-discrete representation of our transmission system. By writing the sampled transmit signal $s(t)$ in a vector $\mathbf{s} \in \mathbb{C}^{N \times 1}$, we can reformulate (1) by

$$\mathbf{s} = \mathbf{G} \mathbf{x}, \quad (3)$$

with

$$\mathbf{G} = [\mathbf{g}_{1,1} \quad \mathbf{g}_{2,1} \quad \cdots \quad \mathbf{g}_{L,1} \quad \mathbf{g}_{1,2} \quad \cdots \quad \mathbf{g}_{L,K}], \quad (4)$$

$$\mathbf{x} = [x_{1,1} \quad x_{2,1} \quad \cdots \quad x_{L,1} \quad x_{1,2} \quad \cdots \quad x_{L,K}]^T. \quad (5)$$

Vector $\mathbf{g}_{l,k} \in \mathbb{C}^{N \times 1}$ represents the sampled basis pulses of (2) and builds the transmit matrix $\mathbf{G} \in \mathbb{C}^{N \times LK}$ while $\mathbf{x} \in \mathbb{C}^{LK \times 1}$ stacks all the transmitted data symbols in a large vector. Let us denote the receive matrix by $\mathbf{Q} = [\mathbf{q}_{1,1} \quad \cdots \quad \mathbf{q}_{L,K}] \in \mathbb{C}^{N \times LK}$ which is similarly defined as the transmit matrix, see (2) and (4), but a different prototype filter $p(t)$ might be used. With a time-variant convolution matrix $\mathbf{H} \in \mathbb{C}^{N \times N}$ the whole transmission system can then be expressed as:

$$\mathbf{y} = \mathbf{Q}^H \mathbf{H} \mathbf{G} \mathbf{x} + \mathbf{n}, \quad (6)$$

where $\mathbf{y} = [y_{1,1} \quad \cdots \quad y_{L,K}]^T \in \mathbb{C}^{LK \times 1}$ represents the received symbols and $\mathbf{n} \sim \mathcal{CN}(\mathbf{0}, P_n \mathbf{Q}^H \mathbf{Q})$ the Gaussian distributed noise. Without loss of generality, we normalize the receive matrix so that $\mathbf{q}_{l,k}^H \mathbf{q}_{l,k} = 1$. In FBMC and pure OFDM, we have $\mathbf{Q} = \mathbf{G}$, while in CP-OFDM the transmit and receive matrix are slightly different, $\mathbf{Q} \neq \mathbf{G}$. Note that the orthogonality condition of OFDM implies that $\mathbf{Q}^H \mathbf{G} = \mathbf{I}_{LK}$ and the real orthogonality condition of FBMC that $\Re\{\mathbf{Q}^H \mathbf{G}\} = \mathbf{I}_{LK}$. In doubly-selective channels, orthogonality no longer holds, leading to interference, described by the off-diagonal elements of $\mathbf{Q}^H \mathbf{H} \mathbf{G}$. The diagonal elements, on the other hand, describe the signal components. To keep the statical investigation simple, see (11)-(13), we utilize the Kronecker product \otimes to rewrite (6) for the received symbol $y_{l,k}$ by

$$y_{l,k} = \mathbf{q}_{l,k}^H \mathbf{H} \mathbf{G} \mathbf{x} + n_{l,k} = \left((\mathbf{G} \mathbf{x})^T \otimes \mathbf{q}_{l,k}^H \right) \text{vec}\{\mathbf{H}\} + n_{l,k}, \quad (7)$$

where $\text{vec}\{\mathbf{H}\}$ denotes the vectorized time-variant convolution matrix. Finally, the estimated data symbols $\hat{x}_{l,k}$ at the receiver are obtained by one-tap equalization, that is,

$$\hat{x}_{l,k} = \mathbf{Q} \begin{Bmatrix} y_{l,k} \\ h_{l,k} \end{Bmatrix}, \quad (8)$$

with $h_{l,k} = \mathbf{q}_{l,k}^H \mathbf{H} \mathbf{g}_{l,k}$ denoting the appropriate diagonal element of $\mathbf{Q}^H \mathbf{H} \mathbf{G}$ and $\mathbf{Q}\{\cdot\}$ the quantization operator, that is, nearest neighbor detection. Most of the energy is concentrated at the diagonal elements of $\mathbf{Q}^H \mathbf{H} \mathbf{G}$, so that one-tap equalizers achieve good performances till some Signal-to-Noise Ratio (SNR) threshold is reached, see Section IV. Furthermore, as long as the interference is dominated by the (Gaussian) noise, one-tap equalizers correspond to the maximum likelihood symbol detection which explains why they are so useful in practice.

III. BIT ERROR PROBABILITY

In this section we present a general method to calculate the BEP for an arbitrary linear modulation technique, described in Section II. We limit ourself to m -QAM and \sqrt{m} -PAM signal constellations because they lead to vertical and horizontal decision boundaries, see Figure 1, allowing us to use the following lemma to calculate the BEP:

Lemma 1: Let y and h be zero mean, correlated, complex-valued, Gaussian random variables, then the Cumulative Distribution Function (CDF) of the complex Gaussian ratio $\frac{y}{h}$ reads

$$\begin{aligned} \text{CDF}_{y/h}(z_R, z_I) &= \Pr \left\{ \left(\Re\left\{ \frac{y}{h} \right\} < z_R \right) \wedge \left(\Im\left\{ \frac{y}{h} \right\} < z_I \right) \right\} = \\ &= \frac{1}{4} + \frac{(z_R - \Re\{\alpha\}) \left(2 \tan^{-1} \left(\frac{z_I - \Im\{\alpha\}}{\sqrt{(z_R - \Re\{\alpha\})^2 + \beta - |\alpha|^2}} \right) + \pi \right)}{4\pi \sqrt{(z_R - \Re\{\alpha\})^2 + \beta - |\alpha|^2}} + \\ &+ \frac{(z_I - \Im\{\alpha\}) \left(2 \tan^{-1} \left(\frac{z_R - \Re\{\alpha\}}{\sqrt{(z_I - \Im\{\alpha\})^2 + \beta - |\alpha|^2}} \right) + \pi \right)}{4\pi \sqrt{(z_I - \Im\{\alpha\})^2 + \beta - |\alpha|^2}}, \end{aligned} \quad (9)$$

with

$$\alpha = \frac{\mathbb{E}\{yh^*\}}{\mathbb{E}\{|h|^2}} \quad \text{and} \quad \beta = \frac{\mathbb{E}\{|y|^2}}{\mathbb{E}\{|h|^2}}. \quad (10)$$

Lemma 1 is obtained by reformulating and combining Equations (10)-(15) of [7]. In many cases we only need the projection onto the real axis, ($z_I \rightarrow \infty$), allowing us to further simplify (9), as shown in [8].

In order to apply Lemma 1 in our transmission system, the received symbols $y_{l,k}$ have to be Gaussian distributed, which is only true, conditioned on the transmitted data symbols \mathbf{x} . Utilizing (7) we straightforwardly calculate the required expectations in (10), conditioned on \mathbf{x} , by

$$\mathbb{E}\{|y_{l,k}|^2 | \mathbf{x}\} = \mathbf{x}^T \left(\mathbf{G}^T \otimes \mathbf{q}_{l,k}^H \right) \mathbf{R}_{\text{vec}\{\mathbf{H}\}} \left(\mathbf{G}^T \otimes \mathbf{q}_{l,k}^H \right)^H \mathbf{x}^* + P_n \quad (11)$$

$$\mathbb{E}\{|h_{l,k}|^2\} = \left(\mathbf{g}_{l,k}^T \otimes \mathbf{q}_{l,k}^H \right) \mathbf{R}_{\text{vec}\{\mathbf{H}\}} \left(\mathbf{g}_{l,k}^T \otimes \mathbf{q}_{l,k}^H \right)^H, \quad (12)$$

$$\mathbb{E}\{y_{l,k} h_{l,k}^* | \mathbf{x}\} = \mathbf{x}^T \left(\mathbf{G}^T \otimes \mathbf{q}_{l,k}^H \right) \mathbf{R}_{\text{vec}\{\mathbf{H}\}} \left(\mathbf{g}_{l,k}^T \otimes \mathbf{q}_{l,k}^H \right)^H, \quad (13)$$

in which $\mathbf{R}_{\text{vec}\{\mathbf{H}\}} = \mathbb{E}\{\text{vec}\{\mathbf{H}\} \text{vec}\{\mathbf{H}\}^H\}$ represents the correlation matrix of the vectorized time-variant convolution matrix and depends on the underlying power delay profile and the Doppler spectral density. We normalize the channel so that it has unit power, that is, the taps of the power delay profile sum up to one. Combining Lemma 1 and (11)-(13) allows us to express the CDF, conditioned on \mathbf{x} , of our transmission system in (8), $\text{CDF}_{y_{l,k}/h_{l,k}}(z_R, z_I | \mathbf{x})$. To calculate the overall BEP, however, we need the CDF conditioned solely on $x_{l,k}$. With a permutation matrix \mathbf{P} we split the transmitted symbols \mathbf{x} into interfering symbols $\mathbf{x}_{l,k} \in \mathcal{A}^{(LK-1) \times 1}$ and the symbol of interest, $x_{l,k}$, according to $\mathbf{x} = \mathbf{P} [\mathbf{x}_{l,k}^T, x_{l,k}]^T$. The required CDF can then be calculated by the law of total probability:

$$\text{CDF}_{y_{l,k}/h_{l,k}}(z_R, z_I | x_{l,k}) = \frac{1}{M} \sum_{\mathbf{x}_{l,k} \in \mathcal{A}^{LK-1}} \text{CDF}_{y_{l,k}/h_{l,k}}(z_R, z_I | \mathbf{x}_{l,k}, x_{l,k}). \quad (14)$$

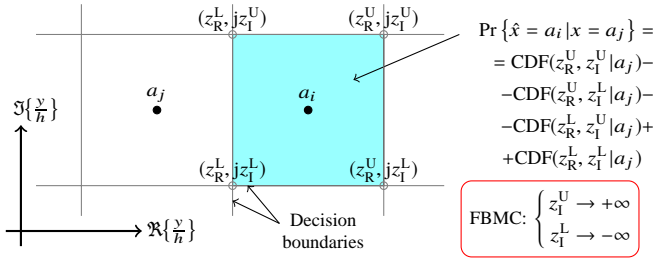


Fig. 1. For a given symbol alphabet \mathcal{A} , we apply Lemma 1 and (11)-(14) to calculate the probability that $\hat{x}_{l,k} = a_i$ is detected, conditioned that $x_{l,k} = a_j$ was sent, allowing us to calculate the BEP in (15).

with $M = |\mathcal{A}^{LK-1}|$ denoting the cardinality. Note that (14) is required to model the interference influence correctly. Many papers, such as [9], assume that the interference is Gaussian distributed, arguing that the central limit theorem can be applied. This is wrong because only few symbols have a significant contribution to the interference, as also shown in [4]. Section IV provides a numerical example of the Gaussian approximation error. For a small symbol alphabet, (14) can be calculated analytically because only a few interferers have a significant contribution which makes the number of summations reasonable small. For higher modulation orders, on the other hand, this is no longer possible because too many summations are required. We then have to rely on numerical approximations, such as Monte Carlo evaluation. Nonetheless, compared to pure simulations we have the advantages of analytical insights and a highly reduced evaluation time.

Finally, with Lemma 1 and (11)-(14) we have all the necessary tools to calculate the BEP of transmit symbol $x_{l,k}$, given by:

$$\text{BEP}_{l,k} = \frac{1}{\log_2 |\mathcal{A}|} \sum_{p=1}^{\log_2 |\mathcal{A}|} \frac{1}{|\mathcal{A}|} \sum_{j=1}^{|\mathcal{A}|} \sum_{a_i \in \mathcal{E}_j^p} \Pr \{ \hat{x}_{l,k} = a_i | x_{l,k} = a_j \}. \quad (15)$$

Set $\mathcal{A} = \{a_1, \dots, a_{|\mathcal{A}|}\}$ describes the symbol alphabet whereas each symbol is mapped to a unique bit sequence of size $\log_2 |\mathcal{A}|$. Set \mathcal{E}_j^p , on the other hand, represents all those elements of \mathcal{A} for which the bit-value at bit-position $p \in \mathbb{N}$ is different from the corresponding bit-value of a_j . Note that the cardinality of \mathcal{E}_j^p is $\frac{|\mathcal{A}|}{2}$. As illustrated in Figure 1, the probability expression $\Pr \{ \cdot \}$ in (15) can be straightforwardly calculated by the CDF, see (14).

Usually the BEP expression in (15) consists of many terms, mainly due to (14). For the important special case of doubly-flat Rayleigh fading, that is, $\mathbf{H} = \bar{h} \mathbf{I}_N$ with $\bar{h} \sim CN(0, 1)$, however, we find compact expressions. For OFDM, the required expectations in (11)-(13) simplify to $\mathbb{E}\{|y_{l,k}|^2 | \mathbf{x}\} = |x_{l,k}|^2 + P_n$, $\mathbb{E}\{|h_{l,k}|^2\} = 1$ and $\mathbb{E}\{y_{l,k} h_{l,k}^* | \mathbf{x}\} = x_{l,k}$, and no longer depend on the surrounding data symbols $\mathbf{x}_{l,k}$, simplifying (14). For Gray-coded 4-QAM, symmetries allow us to rewrite (15) by $\text{BEP}_{l,k} = \text{CDF}_{y_{l,k}/h_{l,k}}(0, \infty | \sqrt{P_x} \frac{1+j}{\sqrt{2}})$ which, together with Lemma 1, leads to:

$$\text{BEP}_{4\text{QAM}} = \frac{1}{2} - \frac{1}{2\sqrt{1 + 2\frac{1}{\text{SNR}}}}, \quad (16)$$

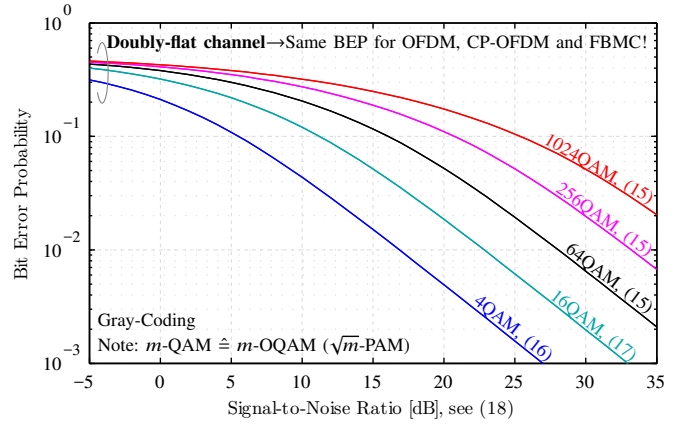


Fig. 2. Doubly-flat fading represents an important special case because it also describes the BEP for a doubly-selective channel as long as the SNR is smaller than a certain threshold, see Figure 3.

identical for each transmit symbol. FBMC experiences imaginary interference. However, this does not influence the BEP for a doubly-flat channel, so that (16) also describes the BEP for 2-PAM FBMC. Similar as before, we find the BEP for 16-QAM respectively 4-PAM by:

$$\text{BEP}_{16\text{Q}} = \frac{1}{2} - \frac{3}{8\sqrt{1 + 10\frac{1}{\text{SNR}}}} - \frac{6}{8\sqrt{9 + 10\frac{1}{\text{SNR}}}} + \frac{5}{8\sqrt{25 + 10\frac{1}{\text{SNR}}}}, \quad (17)$$

For higher modulation orders, similar expressions can be derived but they involve many terms so that we omit them at this point. The SNR in (16) and (17) is defined as:

$$\text{SNR} = \frac{P_x^{\text{OFDM}}}{P_n} = \frac{P_x^{\text{FBMC}}}{\frac{1}{2}P_n}. \quad (18)$$

where $P_x = \mathbb{E}\{|x_{l,k}|^2\}$ represents the average data symbol power. For the same bandwidth FL , setting $P_x^{\text{FBMC}} = \frac{1}{2}P_x^{\text{OFDM}}$, see (18), implies that the average transmit power $P_S = \frac{1}{KT} \int_{-\infty}^{\infty} \mathbb{E}\{|s(t)|^2\} dt$ is the same for OFDM, CP-OFDM and FBMC, allowing a fair comparison. FBMC only experiences half the noise power due to “taking the real part”, which explains the factor of $\frac{1}{2}$ in (18). Furthermore, interpreting (18), we have to keep in mind that the channel has, on average, unit power and that the basis pulses are (real) orthonormal.

The special case of a doubly-flat channel can also be used to approximate the BEP in doubly-selective channels. We simply replace the SNR by the Signal-to-Interference plus Noise Ratio (SINR) in the BEP expressions of a doubly-flat channel. This corresponds to the assumption of Gaussian distributed interference which delivers a rough approximation of the true BEP, see Section IV.

IV. NUMERICAL RESULTS

In this section we investigate the influence of time-variant multipath propagation on OFDM without CP, CP-OFDM and FBMC (Hermite prototype filter [6]). Furthermore, our theoretical derivations of Section III are validated by Monte Carlo simulations and we show the approximation error for the assumption of Gaussian distributed interference. Figure 2 shows the BEP over SNR for the special case of doubly-flat fading. The performance is independent of a specific

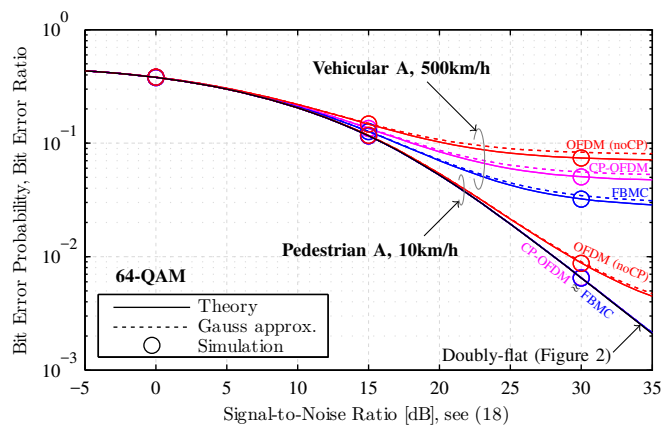


Fig. 3. Simulations validate our BEP calculations of Section III. The interference is not Gaussian distributed, so that the Gaussian approximation only provides a rough estimate of the true BEP.

modulation scheme but we should keep in mind that FBMC has a lower out-of-band emission than OFDM. Furthermore, for the same bandwidth FL , FBMC and OFDM without CP have the same bit rate while the bit rate for CP-OFDM is lower by a factor of $(1 + T_{CP}F)$. Nonetheless, all modulation schemes use the same transmit power P_S , allowing a fair comparison.

For the remaining examples we consider a subcarrier spacing of $F = 15$ kHz, same as in LTE, a Jakes Doppler spectrum and two different channel models: Firstly, the Pedestrian A channel model which has a Root Mean Square (RMS) delay spread of 46 ns. Such small delay spread describes the reality of current (and future) mobile communication systems more accurately than channel models with a much higher delay spread due to various reasons [10]. Secondly, the Vehicular A channel model which has a relatively high RMS delay spread of 370 ns. Although we restrict ourself to these two channel models, it is worth mentioning that the included MATLAB code allows for an arbitrary tapped delay line channel model, so that a large range of possible scenarios can be investigated. The sampling rate is chosen as small as possible but high enough so that it fits approximately the predefined delay taps of the channel model. For a Pedestrian A channel model this leads to a sampling rate of 10.08 MHz and for a Vehicular A model to 2.94 MHz. The BEP is evaluated at the middle position and the number of subcarriers L and the number of multicarrier symbols K are chosen so that they include all significant interferers. Figure 3 shows the BEP over the SNR. As long as the interference is dominated by the noise, the BEP of a doubly-flat channel accurately describes the transmission system. For a Pedestrian A channel model at low velocities, one tap equalizers are sufficient for CP-OFDM and FBMC, but not necessarily for OFDM without CP. The interference in case of a Vehicular A channel at 500 km/h is mainly dominated by the Doppler spread, so that FBMC (with a Hermite prototype filter) performs better than OFDM. For a time-invariant channel, the BEP of CP-OFDM becomes the same as for doubly-flat fading. FBMC, on the other hand, is effected by a relatively high delay spread in a Vehicular A channel, so that it deviates from doubly-flat fading at high SNR values (not shown in the Figure). However, for practical relevant SNR ranges smaller than 20 dB this

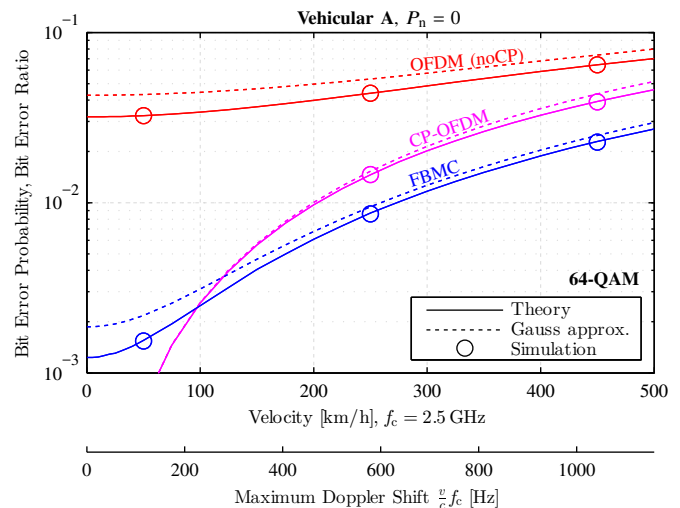


Fig. 4. Similar to Figure 3, simulations validate our BEP expressions. The Gaussian approximation leads to relatively large errors.

is no issue. Figure 4 shows how the BEP depends on the velocity in case of zero noise and a Vehicular A channel model. For low velocities, CP-OFDM shows the lowest BEP because interference caused by frequency-selectivity can be completely eliminated at the expense of a lower bit rate. For velocities higher than 100 km/h, however, FBMC outperforms CP-OFDM due to a better robustness in time-variant channels.

V. CONCLUSION

The derived BEP expressions help to analyze the influence of time-variant multipath propagation in OFDM and FBMC. In highly time-varying channels, FBMC performs better than CP-OFDM because the underlying prototype filter has a better joint time-frequency localization, although both methods suffer from interference in high SNR regimes. Only in highly frequency-selective channels, CP-OFDM outperforms FBMC. However, in many practical cases, the delay spread is so low, that one-tap equalizers achieve good performances in FBMC.

REFERENCES

- [1] B. Farhang-Boroujeny, "OFDM versus filter bank multicarrier," *IEEE Signal Processing Magazine*, vol. 28, no. 3, pp. 92–112, 2011.
- [2] R. Nissel and M. Rupp, "Enabling low-complexity MIMO in FBMC-OQAM," in *IEEE Globecom Workshops (GC Wkshps)*, 2016.
- [3] L. Rugini and P. Banelli, "BER of OFDM systems impaired by carrier frequency offset in multipath fading channels," *IEEE Transactions on Wireless Communications*, vol. 4, no. 5, pp. 2279–2288, 2005.
- [4] T. Wang, J. G. Proakis, E. Masry, and J. R. Zeidler, "Performance degradation of OFDM systems due to Doppler spreading," *IEEE Transactions on Wireless Communications*, vol. 5, no. 6, pp. 1422–1432, 2006.
- [5] H. G. Feichtinger and T. Strohmer, *Gabor analysis and algorithms: Theory and applications*. Springer Science & Business Media, 2012.
- [6] R. Nissel and M. Rupp, "On pilot-symbol aided channel estimation in FBMC-OQAM," in *IEEE ICASSP*, 2016.
- [7] R. J. Baxley, B. T. Walkenhorst, and G. Acosta-Marum, "Complex Gaussian ratio distribution with applications for error rate calculation in fading channels with imperfect CSI," in *IEEE GLOBECOM*, 2010.
- [8] R. Nissel and M. Rupp, "Bit error probability for pilot-symbol aided channel estimation in FBMC-OQAM," in *IEEE ICC*, 2016.
- [9] M. Russell and G. L. Stuber, "Interchannel interference analysis of OFDM in a mobile environment," in *IEEE VTC*, 1995, pp. 820–824.
- [10] H. Asplund, K. Larsson, and P. Okvist, "How typical is the "typical urban" channel model?" in *IEEE VTC*, 2008, pp. 340–343.